Decay of RNA and infectious SARS-CoV-2 and murine hepatitis virus in wastewater

Authors:

Kevin Purves[1], Liam J. Reynolds[2], Laura Sala-Comorera[3], Niamh A. Martin[2], Darren L Dahly[4,5], Wim G. Meijer[2] and Nicola F. Fletcher[1*]

Affiliations:

[1] UCD School of Veterinary Medicine and UCD Conway Institute, University College Dublin, Ireland

[2] UCD School of Biomolecular and Biomedical Science, UCD Earth Institute and UCD Conway Institute, University College Dublin, Ireland

[3]Section of Microbiology, Virology and Biotechnology, Department of Genetics, Microbiology and Statistics, University of Barcelona, Spain

[4]Health Research Board Clinical Research Facility, University College Cork, Ireland

[5]School of Public Health, University College Cork, Ireland

**Corresponding author: Nicola F Fletcher, telephone: +353 (0) 1716 6234, e-mail: nicola.f.fletcher@ucd.ie*

Highlights

1. Infectious SARS-CoV-2 has two phases of decay in wastewater.
2. First phase decay rate for SARS-CoV-2 in wastewater was 9.6 day^{-1} at 4 °C.
3. Infectious SARS-CoV-2 and MHV persisted in wastewater for 7 days at 4 °C.
4. Early decay profiles for infectious SARS-CoV-2 and MHV particles differed in wastewater.

Abstract

Wastewater-based epidemiology (WBE) has been an important tool for population surveillance during the COVID-19 pandemic and continues to play a key role in monitoring SARS-CoV-2 infection levels following reductions in national clinical testing schemes. Studies measuring decay profiles of SARS-CoV-2 in wastewater have underscored the value of WBE, however investigations have been hampered by high biosafety requirements for SARS-CoV-2 infection studies. Therefore, surrogate viruses with lower biosafety standards have been used for SARS-CoV-2 decay studies, such as murine hepatitis virus (MHV), but few studies have directly compared decay rates of both viruses. We compared the persistence of SARS-CoV-2 and MHV in wastewater, using 50 % tissue culture infectious dose ($TCID_{50}$) and reverse transcription quantitative polymerase chain reaction (RT-qPCR) assays to assess infectious virus titre and viral gene markers, respectively. Infectious SARS-CoV-2 and MHV indicate similar endpoints, however observed early decay characteristics differed, with infectious SARS-CoV-2 decaying more rapidly than MHV. We find that MHV is an appropriate infectious virus surrogate for SARS-CoV-2, however inconsistencies exist in viral RNA decay parameters, indicating MHV may not be a suitable nucleic acid surrogate across certain

temperature regimes. This study highlights the importance of sample preparation and the potential for decay rate overestimation in wastewater surveillance for SARS-CoV-2 and other pathogens.

Keywords

SARS-CoV-2, Murine Hepatitis Virus, Wastewater, Persistence, Infectious Virus, Environmental Monitoring

1 Introduction

SARS-CoV-2, a member of the *Coronaviridae* family, is a positive-sense single stranded RNA virus with a genome size of ~30 kb (V'kovski *et al.*, 2021). Responsible for the COVID-19 pandemic, it has caused approximately 7 million confirmed deaths (Smit *et al.*, 2023). The importance of clinical testing to identify infected individuals was a major means of mitigating and controlling outbreaks, as well as informing national strategies which relied on reports of daily cases. The gold standard of clinical testing uses the polymerase chain reaction (PCR) assay to amplify target regions of the SARS-CoV-2 genome from nasopharyngeal or upper respiratory tract swabs of individuals (Lu *et al.*, 2020). Following the development of vaccines, their widespread uptake resulted in many fewer symptomatic cases, hospitalisations and deaths (Bernal *et al.*, 2021; Haas *et al.*, 2021). Consequently, this reduction in symptomatic individuals lowered the number of clinically confirmed cases which in turn diminished the efficiency of clinical testing and contact tracing for population monitoring (Martignoni *et al.*, 2022). However, as SARS-CoV-2 nucleic acid is excreted within faeces of infected individuals, wastewater-based sampling is a powerful, cost-effective tool for SARS-CoV-2 population monitoring, particularly in the absence of case-based detection and surveillance (Bivins, North, *et al.*, 2020; Hart and Halden, 2020; Peccia *et al.*, 2020). This approach uses PCR to quantify SARS-CoV-2 RNA and has so far been deployed in over 72 countries (COVID-19 WBE Collaborative dashboard; www.covid19wbec.org). Further, by sampling the influent of a wastewater treatment plant the prevalence of infections caused by numerous pathogens of concern including Mpox, polio and adenoviruses in its catchment population can be monitored (Lago *et al.*, 2003; Jonge *et al.*, 2022; Martin *et al.*, 2023).

Wastewater monitoring for disease prevalence is a powerful approach strengthened by an understanding of the fate and stability of pathogen targets within sampled matrices (Bogler *et al.*, 2020; La Rosa *et al.*, 2020). Bivins *et al.* (2020) were the first to assess decay rates of SARS-CoV-2 and total RNA in untreated wastewater, highlighting the disparity between infectious virus and RNA quantities in wastewater. Various studies have since reported the decay rates of infectious SARS-CoV-2 RNA in different water matrices, however few reports have measured infectious virus or have used varied incubation conditions and experimental design (Ahmed, Bertsch, Bibby, *et al.*, 2020; Ahmed, Bertsch, Bivins, *et al.*, 2020; Bivins, Greaves, *et al.*, 2020; Chandra *et al.*, 2021; de Oliveira *et al.*, 2021; Hokajärvi *et al.*, 2021; Sala-Comorera *et al.*, 2021; Sherchan *et al.*, 2023). Wastewater experiments using SARS-CoV-2 have also been hampered by high biosafety level requirements, resulting in other *Betacoronavirus* genera being used as surrogates. One such *Betacoronavirus* is the structurally and morphologically similar murine hepatitis virus (MHV) (Ahmed, Bertsch, Bibby, *et al.*, 2020; Ahmed, Bertsch, Bivins, *et al.*, 2020; Gorbalenya *et al.*, 2020; Körner *et al.*, 2020; Canh *et al.*, 2021; Featherstone and Brown, 2022). MHV is a positive-sense single stranded RNA virus with a genome size of ~32 kb (Ye *et al.*, 2016). To date, the only direct comparison of persistence between SARS-CoV-2 and MHV in untreated wastewater from a WWTP (wastewater treatment plant) in Australia compared viral RNA from MHV as a surrogate for SARS-CoV-2 persistence in wastewater (Ahmed, Bertsch, Bibby, *et al.*, 2020). SARS-CoV-2 has also been proposed to exist in different forms in wastewater when assessed using an integrity-based reverse transcription quantitative PCR (RT-qPCR) assay with implications for wastewater-based epidemiology (Wurtzer *et al.*, 2021). The assumption that MHV is a suitable surrogate for wastewater persistence studies requires further

92 investigation and direct comparison with SARS-CoV-2, especially regarding infectivity studies
93 where no comparison has been made.

94 Therefore, the objective of this study was to better characterise and compare the
95 persistence of SARS-CoV-2 and another *Betacoronavirus* (MHV) in wastewater. We used
96 50% tissue culture infectious dose ($TCID_{50}$) and RT-qPCR assays to quantify the decay of
97 infectious virus and RNA, respectively, in human wastewater from an Irish WWTP at
98 environmentally relevant temperatures and timepoints. To assay intact virions following
99 incubation with wastewater, we combined a viability stain with RT-qPCR to assess the
100 impact of capsid integrity on decay rates of virus RNA in wastewater.

101

102 ## 2 Methods

103 ### 2.1 Virus stocks and cell lines

104 An isolate of SARS-CoV-2 (nCoV-Italy-INMI1) was obtained from the European Virus Archive
105 Global (EVAg), with patient written consent and institutional ethical approval (Colavita *et al.*,
106 2020). SARS-CoV-2 was propagated in VeroE6 cells (ATCC CRL-1586) cultured in Dulbecco's
107 Modified Eagle's Medium (DMEM; Gibco) supplemented with 2% heat-inactivated foetal
108 bovine serum (Gibco) as previously described (Purves *et al.*, 2023). Virus used in this study
109 was at passage 3. Murine hepatitis virus (strain A59) was obtained from the American Type
110 Culture Collection (ATCC VR-764) and propagated on murine 17CL1 cells with low glucose
111 DMEM (Gibco) supplemented with 3% each of tryptose phosphate broth (Gibco) and heat-
112 inactivated foetal bovine serum (Gibco).

113 Infectious viral titres of SARS-CoV-2 and MHV were determined using $TCID_{50}$ assays, as
114 previously described (Purves *et al.*, 2023). Wastewater-only controls excluded the possibility

of non-specific cytopathic effect. Briefly, cells were inoculated with a multiplicity of infection of 0.01 for 2 h, washed with PBS, and the medium replaced with DMEM containing 2% foetal bovine serum (Gibco). When cultures exhibited greater than 90% cytopathic effect (CPE), flasks were freeze-thawed three times and supernatants collected and clarified at 3,500 rpm for 30 min at 4 °C. Supernatant was collected, aliquoted and stored at −80 °C. $TCID_{50}$ was determined in VeroE6 or 17CL1 cells in quadruplicate and infectious titre determined using the Reed-Muench method (Reed and Muench, 1938). All work with infectious SARS-CoV-2 was performed at the School of Veterinary Medicine Biosafety Level 3 facility at University College Dublin, Ireland.

2.2 Microcosm design

Microcosm experiments were set up using influent (approx. 500 mL) collected on 2nd August 2021 from the Ringsend WWTP in Dublin, Ireland, which serves 1.9M population equivalents, making it the largest such plant in Ireland (Reynolds et al., 2022). Annual reported physicochemical data has been reported (Uisce Water, 2021) and indicates total suspended solids (243 mg L^{-1}), biochemical oxygen demand (253 mg L^{-1}), total nitrogen (39 mg L^{-1}) and total phosphorous (5 mg L^{-1}). Following collection, influent was stored overnight at 4 °C and resuspended by inversion. Microcosm experiments were established by adding 300 µL SARS-CoV-2 to 2.7 mL aliquots of wastewater (3.16 x 10^4 $TCID_{50}$ mL^{-1}) under BSL-3 conditions, or 300 µL MHV to 2.7 mL aliquots of wastewater (2.15 x 10^4 $TCID_{50}$ mL^{-1}) under BSL-2 conditions, for a final volume of 3 mL per microcosm. The spiked influent microcosms were then incubated at either 4 ± 2 °C, 10 ± 2 °C or room temperature (20 ± 2 °C) in the dark. Samples were collected and stored at -80 °C at specific time points including:

immediately after virus addition, or following incubation at 4 h, 8 h, and 24 h, and every 24 h for 7 days. At the end of the experiment, samples were thawed and centrifuged at 3500 x g for 10 minutes, followed by filtration of the supernatant through a 0.45 µm filter (SFCA low binding filter). Microcosms consisted of two biological replicates, with three technical replicates taken from each.

2.3 Viability assay

Propidium monoazide (PMA) is an intercalating dye with a photo-inducible azide group that can covalently bind to nucleic acids preventing their amplification during PCR. When used as a pre-treatment before RNA extraction, theoretically only “unprotected” nucleic acids are bound. As such it can be used to determine viability in combination with the RT-qPCR assays as only encapsulated RNA will be amplified (Nocker *et al.*, 2007; Fittipaldi *et al.*, 2010). Lyophilised PMA was obtained from Biotium (1 mg; CA, USA) before being made up to a 20 mM master stock using PCR grade H_20. PMA (50 µM final conc.) was added to 140 µL of each sample. The samples were then incubated in the dark for 30 minutes on ice. All samples were then placed in a LED Photolysis device (GenIUL PhAST Blue, IUL Instruments, Spain) for 15 minutes to activate the dye and bind ‘’unprotected’’ nucleic acid in the sample. Viral RNA was extracted immediately as described in Section 2.4.

2.4 Viral nucleic acid extraction and RT-qPCR analysis

SARS-CoV-2 and MHV RNA were extracted from 140 µL of each microcosm using the QIAamp Viral RNA Mini Kit (Qiagen, Germany). RNA extraction controls were included (positive: SARS-CoV-2 viral stock and negative: PCR grade water). RT-qPCR assays were performed on the Roche Lightcycler 96 platform (Roche Diagnostics, Germany) in a total volume of 20 µL, containing 5 µL of template using LightCycler Multiplex RNA Virus Master (Roche Diagnostics, Germany). Primer sequences, concentrations and thermal cycling conditions for each gene are given in Supplementary Table 1 (Besselsen, Wagner and Loganbill, 2002; Lu *et al.*, 2020). All biological sample replicates and RNA extraction controls were analysed in triplicate, with four triplicate quantification standards included in each 96-

well plate, extraction and negative controls were included. Results were expressed as gene copies per millilitre (gc mL^{-1}), and reaction efficiencies for each assays were determined as previously described (Reynolds *et al.*, 2022).

2.5 Data analysis

Decay rates were determined through first-order decay models (Chick, 1908) and a biphasic decay models.

First-order decay rate constants were calculated using the following formulas:

$$N_t = N_0 e^{-kt}$$

$$Ln(N_t/N_0) = -kt$$

Where N_t and N_0 are the $TCID_{50}$ titre and gc mL^{-1} concentrations in the microcosm at time t and time 0, and k is the decay rate. The biphasic decay model was modelled using the following formula:

$$N_t = N_{f0} e^{-k_f t} + N_{s0} e^{-k_s t}$$

Where N_t is the concentration/titre at time t, N_{f0} is the initial concentration/titre of the first decay period and N_{s0} is the concentration of the subsequent decay period. k_f and k_s are the initial and subsequent decay rates. The model fit was assessed by r^2 and RMSE, and the best fitting model was chosen using the Akaike's Information Criterion (AICc), which accounts for model deviance and input parameters.

The time taken for a 90% reduction in initial concentration/titre (T_{90}) was determined as follows:

187 $$T_{90} = \frac{-\ln(0.1)}{k}$$

188 Prism9 (GraphPad Software, USA) was used to perform the statistical analyses and to
189 prepare data plots.

190

191 **2.6 Linear mixed-effects model**

192 A linear mixed-effects model was employed to determine whether the results were
193 influenced by any of the experimental factors inherent within this microcosm approach. The
194 distribution of total RNA was visually inspected across experimental groups, replicates and
195 time. The degree of similarity among technical replicates of each biological sample at each
196 time point was evaluated using the intraclass correlation coefficient (ICC) based on the
197 variance components estimated using a linear mixed-effects model (Bates *et al.*, 2015).
198 Based on the result (ICC > 0.98), the decision was made to simplify subsequent modelling by
199 averaging over the technical replicates within each biological replicate.

200 To estimate the effects of the experimental factors on the total RNA, we also used
201 linear mixed-effects models (Bates *et al.*, 2015) with log-transformed total RNA as the
202 dependent variable; fixed effects for virus, temperature, PMA treatment, and linear time
203 (hours); and a random effect to account for the clustering of multiple observations for each
204 biological replicate over time. This model also allowed us to include samples that were
205 missing values at one or more time points. We then estimated an additional mixed-effects
206 model that added all two-way interactions, and another that only retained two-way
207 interactions with an F-test p-value < 0.10 based on single term deletion (Kuznetsova,
208 Brockhoff and Christensen, 2017).

To compare the decay kinetics of infectious virus, a Wilcoxon rank-sum test was performed. Furthermore, the decay rates of infectious virus and RNA were compared using a Kruskal-Wallis test ($\alpha = 0.05$ for both tests). These tests and the linear mixed effects models were completed using R (Version 4.3.3).

3 Results

3.1 Infectious SARS-CoV-2 decays more rapidly than MHV in wastewater

To determine the persistence of SARS-CoV-2 and MHV in wastewater, the decay rate of infectious virus was quantified under various conditions. A biphasic decay pattern was observed for infectious SARS-CoV-2, with rapid decay observed 8 hours post-inoculation (hpi) at all evaluated temperatures (Figure 1a). During this period, the time required for the infectious titre to be reduced by 90% (T_{90}) ranged between 4.4 – 7.8 hours (with decay rates between 6.08 ± 1.79 and 9.7 ± 3.99 day^{-1}). Following the initial drop in SARS-CoV-2 infectious titre at 10 °C, the rate of decay slowed before falling again after 3 days post infection (dpi) and was undetectable at 4 dpi. At room temperature, infectious SARS-CoV-2 exhibited a slower decay in the first phase, followed by a more rapid decay in the second phase and was also not detectable beyond 4 dpi. The overall decay rates for infectious SARS-CoV-2 during the second phase of decay ranged between 1.54 ± 0.47 and 1.98 ± 0.25 day^{-1} (Figure 1c) Table 2). Interestingly, low levels of infectious SARS-CoV-2 persisted in wastewater at 4 °C until the end of the study period with the slowest rate of decay (1.54 ± 0.47 day^{-1}) following the initial 8-hour decay rate (9.55 ± 3.97 day^{-1}). Infectious MHV was more stable than SARS-CoV-2 for all timepoints up to 8 hpi, and the stability of infectious MHV incubated at 4 and 10 °C remained stable until 2 dpi. Interestingly, at 10 °C, infectious

MHV was reduced at 3 dpi and undetectable 4 dpi, indicating a rapid phase of decay over that period (Figure 1b). This rapid decay after a period of stability fit a biphasic decay model. Titres of MHV maintained at room temperature dropped rapidly after 4 hpi, and no infectious virus was detectable 4 dpi (Figure 1b). The overall decay rates across infectious MHV temperature treatments were lower than for SARS-CoV-2 and ranged between 0.24 ± 0.78 and 1.9 ± 0 day^{-1} Table 2). Of note is the difference in MHV decay patterns (Figure 1d), which were determined as monophasic at 4 °C and room temperature, but biphasic at 10 °C – although this is likely driven by the near total loss of infectious titre 2 dpi. After 5 dpi in wastewater, titres of both viruses remained detectable at 4 °C with similar endpoints at 10°C and room temperature. The infectious titre kinetics and the T_{90} values for both viruses were compared using a Wilcoxon rank-sum test and a Kruskal-Wallis test, respectively. No statistically significant differences across the temperature regimes.

3.2 Decay rates of viral RNA in wastewater

As this water was collected during the pandemic, we confirmed that low level SARS-CoV-2 RNA was present prior to spiking with virus (3.3 gc mL^{-1}), which we considered to be negligible. In contrast to the decay rates of infectious SARS-CoV-2 and MHV, the decay rates of genomic markers for each virus, SARS-CoV-2 N1 and MHV M genes, as quantified from total RNA, were more stable (Figure 2). Total SARS-CoV-2 RNA at 4 °C had a T_{90} of 16.8 ± 2.4 days with a slow decay profile (1.5 ± 2.2 day^{-1}), decay rates were similar at 10 °C (1.5 ± 1.8 day^{-1}, T_{90} = 4.9 ± 3.9 days)(Figure 3a). In contrast, decay rates were higher at room temperature (2.2 ± 2.2 day^{-1}, T_{90} = 3.8 ± 5.3 days). Total MHV RNA had very similar decay rates across all temperatures (between 1.1 ± 2.7 and 1.2 ± 2.6 day^{-1}), however there was

255 more variation in T_{90} values across the different temperature regimes (ranging between 5.7
256 ± 14.8 and 11.6 ± 39.5 days)(Figure 3b). Total SARS-CoV-2 N1 gene levels were higher than
257 MHV M gene, which likely reflects the slightly higher titre of infectious SARS-CoV-2 spiked
258 into the wastewater. While total RNA represents all free extracted RNA within a sample, we
259 also investigated whether RNA that is 'protected' within intact virions can be detected by
260 treating concentrated wastewater samples with PMA (a photo-reactive nucleic acid binding
261 dye) before RNA extraction. PMA-treated samples had an average (3.8 ± 0.6 $\log_{10}$) reduction
262 in the quantifiable gene markers of both viruses compared to matched untreated samples
263 quantifying total RNA (Figure 2 – dashed lines). When the PMA-treated and untreated data
264 at each timepoint was expressed as a percentage, it indicated that less than 5 % of the total
265 viral RNA was protected for SARS-CoV-2 and less than 4 % was protected for MHV. The k_{mean}
266 in PMA-treated samples at 4 and 10 °C were negative compared to untreated samples,
267 which indicates stability in wastewater for the duration of the study – at room temperature
268 the k_{mean} was comparable with untreated samples (1.4 ± 2.0 day^{-1}). The resulting T_{90} values
269 (derived from the decay curve slope) demonstrated sample decay over time. This decay rate
270 increased in PMA-treated SARS-CoV-2 RNA with the biggest increases at 4 °C and 10 °C (21.9
271 ± 533.0 and 14.3 ± 28.0 day^{-1}, respectively). On average, no decay (k_{mean}) was observed in
272 PMA-treated MHV RNA relative to the untreated samples at all temperatures. However,
273 although the decay rates indicate stability, the T_{90} values range was similar for total and
274 PMA-treated MHV RNA (T_{90} = 5.7 ± 22.8 and 11.8 ± 36.3).

275 Results of the linear mixed effect models revealed that the only notable interaction was
276 between PMA treatment and virus, suggesting that PMA influenced total RNA in SARS-CoV-2
277 samples less than it did in MHV samples. Notably, there were no interactions suggesting
278 that the rate of decay varied across any experimental factors. The T_{90} values for viral RNA

(untreated and PMA-treated) for both viruses were compared using a Kruskal-Wallis test. Notably, these results indicate statistically significant differences only at room temperature between these two viruses (**Error! Reference source not found.**).

4 Discussion

The persistence of SARS-CoV-2 and MHV (RNA and infectious virus) was compared in wastewater at different temperatures. Rapid initial decay of infectious SARS-CoV-2 was observed at early timepoints followed by a slower decay profile with a bi-phasic decay model fitting our observations better than monophasic decay. Interestingly Bivins *et al.* (2020), who also described a rapid early (<10 hpi) phase of decay, stated a biphasic model did not improve the fit compared to a monophasic (first order) decay model. Rapid early decay and monophasic decline was also noted more recently by Sherchan *et al.* (2023), who had a comparable microcosm and indicated a T_{90} of <11 hpi in raw wastewater. The difference in decay kinetics could reflect unknown differences in the wastewater matrices used in each study, such as the potential impacts of freezing and thawing wastewater before assessing decay rates or concentrations in spiked virus (Bivins, Greaves, *et al.*, 2020). The observed T_{90} values of infectious MHV aligns with the findings of Ye *et al.* (2016) across a similar temperature range (0.5 to 1.5 days). Longer T_{90} periods have been noted for MHV in pasteurised settled sewage (3 and 35 days at 4 °C and 25 °C, respectively), as reported by Casanova *et al.* (2009), who hypothesised that the pasteurisation process reduced the 'proteolytic activity' - which would increase viral decay rates in untreated wastewater, as we observed. By comparing the infectious titre kinetics and T_{90} values, our results indicate no statistically significant differences between the two viruses at any temperature. This was an

unexpected result given the apparent contrast in decay phases associated with each virus, nevertheless this finding further suggests that MHV is a suitable infectious virus surrogate for decay studies in wastewater.

MHV and SARS-CoV-2 are structurally similar, with ultrastructural studies reporting average virion diameters of 85 nm for MHV (Bárcena *et al.*, 2009) and 90 nm for SARS-CoV-2 (Klein *et al.*, 2020). Structural components for both viruses include transmembrane proteins, nucleoproteins and large surface glycoproteins, which are anchored to the envelope and commonly referred to as spike (S) proteins. Domains on the spike proteins recognise surface receptors (CEACAM1a and ACE2 for MHV and SARS-CoV-2, respectively) on susceptible cells, which mediate membrane fusion and viral entry (Hoffmann *et al.*, 2020; Shang *et al.*, 2020). Due to the external nature of spike on both coronaviruses in this study, the proteolytic activity of wastewater on this protein may vary with each virus (i.e. structural differences (Chan *et al.*, 2006)) and be involved in our observed differences between infectious viruses. The effects of low pH have previously been shown to lower the infectivity of MHV by driving an irreversible conformational change to the spike (Eifart *et al.*, 2007), this is not the case with infectious SARS-CoV-2 which is stable over a wide pH range (3 – 10) at room temperature (Chin *et al.*, 2020), however previous wastewater studies seem to indicate a narrow pH range even across different regions and treatment plants (7.3 – 8.3) (Casanova *et al.*, 2009; Ye *et al.*, 2016; Bivins, Greaves, *et al.*, 2020; Ahmed *et al.*, 2021; Hokajärvi *et al.*, 2021) – indeed measurements of influent characteristics from the sampled period indicate a pH value of 7.3, falling within this range (Uisce Water, 2021). Additionally, the membrane thickness could play an important role, where SARS-CoV-2 was found to have an average thickness for a biological membrane (4 nm (Klein *et al.*, 2020)), conversely MHV virions have

a remarkably thick membrane (7-8 nm) (Bárcena *et al.*, 2009), which could explain our findings where infectious MHV initially remained stable for 2 days longer than SARS-CoV-2.

The decay of SARS-CoV-2 and MHV RNA was characterised and as expected based on previous studies (Bivins, Greaves, *et al.*, 2020; Sala-Comorera *et al.*, 2021), revealed slower decay rates than that of infectious virus. In addition, temperature is well known to impact virus stability in wastewater, and therefore the increased rates of decay with increasing temperature is unsurprising and has previously been shown in fresh- and saltwater (Sala-Comorera *et al.*, 2021), and wastewater (Wurtzer *et al.*, 2021). The overall stability of viral RNA in wastewater is not a novel finding, however, our observations do reveal a shorter period of time for the SARS-CoV-2 RNA levels to be reduced by 90% when compared with similar studies and incubation temperatures (Ahmed, Bertsch, Bibby, *et al.*, 2020; Hokajärvi *et al.*, 2021). For example, Ahmed *et al.* (2020) found that SARS-CoV-2 RNA at 4 °C had a T_{90} value of 27.8 days, over 10 days longer than the present study. As already mentioned, this variability is most likely due to the different wastewater matrices, for example wastewater biofilms are suggested to increase persistence of viruses (Skraber *et al.*, 2007). Alternatively, in our study wastewater microbes may have influenced viral RNA persistence (Rzezutka and Cook, 2004; Sala-Comorera *et al.*, 2021). Recent studies also suggest that enteric viruses and SARS-CoV-2 utilise vesicles to increase persistence (Mirabelli and Wobus, 2018; Santiana *et al.*, 2018; Xia *et al.*, 2023). Therefore, although the SARS-CoV-2 preparation of Ahmed *et al*. (2020) was irradiated beforehand (to facilitate work at BSL-2), potential virion-laden vesicles could protect and extend persistence. Notably, Hokajärvi *et al.* (2021) estimated T_{90} values 2-3 times longer than our measurements, depending on the SARS-CoV-2 genomic target (E-Sarbeco or N2 gene, respectively), indicating a potentially large disparity in results. Collectively these results urge careful consideration when selecting biomarkers or when

adopting decay rates. For example, Mcmahan *et al.* (2021) incorporated decay values from Ahmed *et al.* (2020) into a susceptible-exposed-infectious-recovered (SEIR) model to estimate SARS-CoV-2 infected populations in South Carolina, USA, however a shorter decay rate (as presented here) would likely influence predictions about viral persistence and transport, impacting conclusions of such studies.

The MHV RNA decay rates reported in the present study differed in some respects from the literature, with Ahmed *et al.* (2020) reporting longer T_{90} values, especially at lower temperatures. At higher temperatures, however, our findings reflected those of Chandra *et al.* (2021). Interestingly, Ahmed *et al.* (2020) found that the overall T_{90} range of MHV RNA (17.3 to 56.6 days) was longer than SARS-CoV-2 RNA (12.6 to 27.8 days), indicating that SARS-CoV-2 decays faster than MHV across the temperatures evaluated. We observed that over similar temperature ranges to those evaluated by Ahmed *et al.* (2020) the overall T_{90} values are similar between SARS-CoV-2 RNA (3.8 ± 5.3 to 16.8 ± 2.4 days) and MHV RNA (5.7 ± 14.8 to 11.6 ± 39.5 days). As the same genomic targets were used in each study (SARS-CoV-2 N1 gene and MHV M gene), the reason for the overall difference in T_{90} values is unclear.

Samples were also treated before RNA extraction with a photo-reactive dye which binds to nucleic acid, yielding insights into the decay of 'protected' RNA within intact virions. The $\log_{10}$ reduction of both gene biomarkers indicates a large proportion of target RNA is available immediately for binding by the photo-reactive dye. When the treated and untreated data is expressed as a percentage, it indicates that less than 5 % of the total viral RNA from either virus was protected. Samples were frozen before PMA-treatment, and although freezing wastewater samples before PMA-treatment has been shown to have little

or no effect (Fuster *et al.*, 2016), this may have had an impact on capsid integrity. Alternatively, the nature of the virus preparation used in this study, in which virions are released from infected cells by freeze-thawing, may have generated a population of viruses in various states of assembly, with a fraction of the viral genomes successfully replicated but unpackaged and therefore available for binding by the photo-reactive dye (Boersma *et al.*, 2020; Scherer *et al.*, 2021). These factors may have affected virus capsid integrity, however these percentage findings reflect a similar study, where >10 % of SARS-CoV-2 RNA was protected from amplification (Wurtzer *et al.*, 2021). Furthermore, the T_{90} values derived from PMA-treated samples were longer at lower temperatures (4 and 10 °C for SARS-CoV-2 and 4 °C for MHV). Therefore at lower temperatures, T_{90} values derived from untreated samples may overestimate the decay of viral gene biomarkers, which may have implications when these values are incorporated into spatial or SEIR models (Mcmahan *et al.*, 2021; Robins *et al.*, 2022). This is a crucial distinction to make, given that intact virus particles and free viral RNA pose different risks when assessing impacts to human health (or other concerns, such as food security). It is therefore important to consider sample treatment and the detected forms of viral nucleic acid in certain wastewater-based epidemiological studies and how results should be interpreted (Wurtzer *et al.*, 2021). Furthermore, by comparing the decay metrics (T_{90}), the only significant differences were at room temperature (regardless of treatment) and at 10 °C. These findings are inconsistent and contradict previous studies, potentially suggesting that MHV is only a suitable nucleic acid surrogate at colder temperatures. Additionally, our results emphasise that a PMA-based capsid integrity assay does not serve as an appropriate substitute for gauging infectious virus, as assessed through a cell-based assay. We attribute this to the inherent complexities of the latter, including virus-to-cell interactions and other variables which lead to observable cytopathic

effects, in contrast to the direct amplification of a PCR assay. PMA-treatment does reduce non-target amplification – which may be more informative than standard PCR approaches when isolating infectious virus or cell-based assays are impractical (Wurtzer *et al.*, 2021).

Limitations of our study include potential loss of virus in solids following centrifugation of wastewater prior to extraction. However, previous studies have not reported a significant relationship between solids and adsorbed virus, and have indicated that >90 % of SARS-CoV-2 RNA remains detectable in the liquid phase (Ye *et al.*, 2016; de Oliveira *et al.*, 2021; Weidhaas *et al.*, 2021). Additionally, there were quantifiable levels of SARS-CoV-2 RNA in the wastewater used, although these concentrations were low and considered to have had a negligible impact on the study.

In conclusion, we have directly compared the decay of RNA and infectious SARS-CoV-2 and MHV in untreated wastewater at environmentally relevant temperatures. While both viruses exhibited similar endpoints, the rapid initial decay of infectious SARS-CoV-2 contrasts with the more stable profile of MHV. Despite these observations, our data indicates that MHV is a suitable surrogate for infectious SARS-CoV-2 at all temperatures evaluated, but only at 4°C as a nucleic acid surrogate. Additionally, our study highlights the complexities of evaluating viral decay in wastewater matrices and presents methodological considerations for future virus decay studies.

Declaration of Interest Statement

The authors declare that they have no known competing financial interests or personal relationships that could have appeared to influence the work reported in this paper.

418

419 **Author Contributions Statement**

420 KP, LJR, LSC, WM and NF designed the experiments. KP and LJR carried out initial
421 experimentation. KP and NF set up the microcosm. KP carried out RNA extractions,
422 performed RT-PCRs and TCID50 assays. All authors contributed to data analysis. All authors
423 contributed to the article and approved the submitted version.

424

425 **Acknowledgements**

426 This research was funded by a Science Foundation Ireland COVID-19 Rapid Response Grant
427 (20-COV-8460).

428

429 **References**

430 Ahmed, W., Bertsch, P. M., Bivins, A., *et al.* (2020) 'Comparison of virus concentration
431 methods for the RT-qPCR-based recovery of murine hepatitis virus , a surrogate for SARS-
432 CoV-2 from untreated wastewater', *Science of the Total Environment*. Elsevier B.V.,
433 739(June), p. 139960. doi: 10.1016/j.scitotenv.2020.139960.

434 Ahmed, W., Bertsch, P. M., Bibby, K., *et al.* (2020) 'Decay of SARS-CoV-2 and surrogate
435 murine hepatitis virus RNA in untreated wastewater to inform application in wastewater-
436 based epidemiology', *Environmental Research*. Elsevier Inc., 191(August), p. 110092. doi:
437 10.1016/j.envres.2020.110092.

438 Ahmed, W. *et al.* (2021) 'Comparative decay of culturable faecal indicator bacteria,
439 microbial source tracking marker genes, and enteric pathogens in laboratory microcosms

that mimic a sub-tropical environment', *Science of the Total Environment*. Elsevier B.V., 751, p. 141475. doi: 10.1016/j.scitotenv.2020.141475.

Bárcena, M. *et al.* (2009) 'Cryo-electron tomography of mouse hepatitis virus: Insights into the structure of the coronavirion', *Proceedings of the National Academy of Sciences of the United States of America*, 106(2), pp. 582–587. doi: 10.1073/pnas.0805270106.

Bates, D. *et al.* (2015) 'Fitting linear mixed-effects models using lme4', *Journal of Statistical Software*, 67(1). doi: 10.18637/jss.v067.i01.

Bernal, J. L. *et al.* (2021) 'Effectiveness of the Pfizer-BioNTech and Oxford-AstraZeneca vaccines on covid-19 related symptoms, hospital admissions, and mortality in older adults in England: Test negative case-control study', *The BMJ*, 373. doi: 10.1136/bmj.n1088.

Besselsen, D. G., Wagner, A. M. and Loganbill, J. K. (2002) 'Detection of Rodent Coronaviruses by Use of Fluorogenic Reverse Transcriptase-Polymerase Chain Reaction Analysis', 52(2), pp. 111–116.

Bivins, A., Greaves, J., *et al.* (2020) 'Persistence of SARS-CoV-2 in Water and Wastewater', *Environmental Science and Technology Letters*, 7(12), pp. 937–942. doi: 10.1021/acs.estlett.0c00730.

Bivins, A., North, D., *et al.* (2020) 'Wastewater-Based Epidemiology: Global Collaborative to Maximize Contributions in the Fight Against COVID-19', *Environmental Science & Technology*, (54), pp. 7754–7757. doi: 10.1021/acs.est.0c02388.

Boersma, S. *et al.* (2020) 'Translation and Replication Dynamics of Single RNA Viruses', *Cell*, 183(January), pp. 1–16.

Bogler, A. *et al.* (2020) 'Rethinking wastewater risks and monitoring in light of the COVID-19

462 pandemic', *Nature Sustainability*. Springer US, 3(12), pp. 981–990. doi: 10.1038/s41893-020-
463 00605-2.

464 Canh, V. D. *et al.* (2021) 'Capsid integrity RT-qPCR for the selective detection of intact SARS-
465 CoV-2 in wastewater', *Science of the Total Environment*. The Authors, 791, p. 148342. doi:
466 10.1016/j.scitotenv.2021.148342.

467 Casanova, L. *et al.* (2009) 'Survival of surrogate coronaviruses in water', *Water Research*.
468 Elsevier Ltd, 43(7), pp. 1893–1898. doi: 10.1016/j.watres.2009.02.002.

469 Chan, W.-E. *et al.* (2006) 'Functional Characterization of Heptad Repeat 1 and 2 Mutants of
470 the Spike Protein of Severe Acute Respiratory Syndrome Coronavirus', *Journal of Virology*,
471 80(7), pp. 3225–3237. doi: 10.1128/jvi.80.7.3225-3237.2006.

472 Chandra, F. *et al.* (2021) 'Persistence of Dengue (Serotypes 2 and 3), Zika, Yellow Fever, and
473 Murine Hepatitis Virus RNA in Untreated Wastewater', *Environmental Science and*
474 *Technology Letters*, 8(9), pp. 785–791. doi: 10.1021/acs.estlett.1c00517.

475 Chick, H. (1908) *An investigation of the laws of disinfection*, *Journal of Hygiene*. doi:
476 10.1017/S0022172400006987.

477 Chin, A. W. H. *et al.* (2020) 'Stability of SARS-CoV-2 in different environmental conditions',
478 *The Lancet Microbe*. Elsevier Ltd, 1(1), p. e10. doi: 10.1016/S2666-5247(20)30003-3.

479 Colavita, F. *et al.* (2020) 'Virological Characterization of the First 2 COVID-19 Patients
480 Diagnosed in Italy : Phylogenetic Analysis , Virus Shedding Profile From Different Body Sites ,
481 and Antibody Response Kinetics', *Open Forum Infectious Diseases*, 7(10), pp. 1–8. doi:
482 10.1093/ofid/ofaa403.

483 Eifart, P. *et al.* (2007) 'Role of Endocytosis and Low pH in Murine Hepatitis Virus Strain A59

Cell Entry', *Journal of Virology*, 81(19), pp. 10758–10768. doi: 10.1128/jvi.00725-07.

Featherstone, A. B. and Brown, C. (2022) 'Murine Hepatitis Virus , a Biosafety Level 2 Model for SARS-CoV- 2 , Can Remain Viable on Meat and Meat Packaging Materials for at Least 48 Hours', *ASM Microbiology Spectrum*. American Society for Microbiology, 10(5), pp. 1–11. doi: 10.1128/spectrum.01862-22.

Fittipaldi, M. *et al.* (2010) 'Discrimination of infectious bacteriophage T4 virus by propidium monoazide real-time PCR', *Journal of Virological Methods*, 168(1–2), pp. 228–232. doi: 10.1016/j.jviromet.2010.06.011.

Fuster, N. *et al.* (2016) 'Propidium monoazide RTqPCR assays for the assessment of hepatitis A inactivation and for a better estimation of the health risk of contaminated waters', 101, pp. 226–232. doi: 10.1016/j.watres.2016.05.086.

Gorbalenya, A. E. *et al.* (2020) 'The species Severe acute respiratory syndrome-related coronavirus: classifying 2019-nCoV and naming it SARS-CoV-2', *Nature Microbiology*, 5(4), pp. 536–544. doi: 10.1038/s41564-020-0695-z.

Haas, E. J. *et al.* (2021) 'Impact and effectiveness of mRNA BNT162b2 vaccine against SARS-CoV-2 infections and COVID-19 cases, hospitalisations, and deaths following a nationwide vaccination campaign in Israel: an observational study using national surveillance data', *The Lancet*. Elsevier Ltd, 397(10287), pp. 1819–1829. doi: 10.1016/S0140-6736(21)00947-8.

Hart, O. E. and Halden, R. U. (2020) 'Computational analysis of SARS-CoV-2/COVID-19 surveillance by wastewater-based epidemiology locally and globally : Feasibility , economy , opportunities and challenges', *Science of the Total Environment*. The Authors, 730, p. 138875. doi: 10.1016/j.scitotenv.2020.138875.

506 Hoffmann, M. *et al.* (2020) 'SARS-CoV-2 Cell Entry Depends on ACE2 and TMPRSS2 and Is
507 Blocked by a Clinically Proven Protease Inhibitor', *Cell*, 181(2), pp. 271-280.e8. doi:
508 10.1016/j.cell.2020.02.052.

509 Hokajärvi, A. M. *et al.* (2021) 'The detection and stability of the SARS-CoV-2 RNA biomarkers
510 in wastewater influent in Helsinki, Finland', *Science of the Total Environment*. The Authors,
511 770, p. 145274. doi: 10.1016/j.scitotenv.2021.145274.

512 Jonge, E. F. De *et al.* (2022) 'The detection of monkeypox virus DNA in wastewater samples
513 in the Netherlands', *Science of the Total Environment*, 852(August), pp. 48–51. doi:
514 10.1016/j.scitotenv.2022.158265.

515 Klein, S. *et al.* (2020) 'SARS-CoV-2 structure and replication characterized by in situ cryo-
516 electron tomography', *Nature Communications*. Springer US, 11(1), pp. 1–10. doi:
517 10.1038/s41467-020-19619-7.

518 Körner, R. W. *et al.* (2020) 'Of Mice and Men : The Coronavirus MHV and Mouse Models as a
519 Translational Approach to', *MDPI Viruses*, 12(880), pp. 1–26. doi: 10.3390/v12080880.

520 Kuznetsova, A., Brockhoff, P. B. and Christensen, R. H. B. (2017) 'lmerTest Package: Tests in
521 Linear Mixed Effects Models', *Journal of Statistical Software*, 82(13), pp. 1–26. doi:
522 10.18637/JSS.V082.I13.

523 Lago, P. M. *et al.* (2003) 'Poliovirus detection in wastewater and stools following an
524 immunization campaign in Havana , Cuba', pp. 772–777. doi: 10.1093/ije/dyg185.

525 Lu, X. *et al.* (2020) 'US CDC real-time reverse transcription PCR panel for detection of severe
526 acute respiratory syndrome Coronavirus 2', *Emerging Infectious Diseases*, 26(8), pp. 1654–
527 1665. doi: 10.3201/eid2608.201246.

528 Martignoni, M. M. *et al.* (2022) 'Downsizing of COVID-19 contact tracing in highly immune
529 populations', pp. 1–13. doi: 10.1371/journal.pone.0268586.

530 Martin, N. A. *et al.* (2023) 'Human Adenovirus F41 in Wastewater during Outbreak of Severe
531 Acute Hepatitis', *Emerging Infectious Diseases*, 29(4), pp. 751–760.

532 Mcmahan, C. S. *et al.* (2021) 'COVID-19 wastewater epidemiology: a model to estimate
533 infected populations', *Lancet Planet Health*, 5(12), pp. 874–881.

534 Mirabelli, C. and Wobus, C. E. (2018) 'All Aboard! Enteric Viruses Travel Together', *Cell Host
535 and Microbe*. Elsevier Inc., 24(2), pp. 183–185. doi: 10.1016/j.chom.2018.07.012.

536 Nocker, A. *et al.* (2007) 'Use of propidium monoazide for live/dead distinction in microbial
537 ecology', *Applied and Environmental Microbiology*, 73(16), pp. 5111–5117. doi:
538 10.1128/AEM.02987-06.

539 de Oliveira, L. C. *et al.* (2021) 'Viability of SARS-CoV-2 in river water and wastewater at
540 different temperatures and solids content', *Water Research*, 195(May), p. 117002. doi:
541 10.1016/j.watres.2021.117002.

542 Peccia, J. *et al.* (2020) 'Measurement of SARS-CoV-2 RNA in wastewater tracks community
543 infection dynamics', *Nature Biotechnology*. Springer US, 38(October). doi: 10.1038/s41587-
544 020-0684-z.

545 Purves, K. *et al.* (2023) 'A novel antiviral formulation containing caprylic acid inhibits SARS-
546 CoV-2 infection of a human bronchial epithelial cell model', *The Journal of general virology*,
547 104(2), pp. 1–12. doi: 10.1099/jgv.0.001821.

548 Reed, L. J. and H. Muench (1938) 'A simple method of estimating fifty per cent endpoints',
549 *The American Journal of Hygiene*, 27(3), pp. 493–497. doi:

10.7723/antiochreview.72.3.0546.

Reynolds, L. J. *et al.* (2022) 'SARS-CoV-2 variant trends in Ireland: Wastewater-based epidemiology and clinical surveillance', *Science of The Total Environment*. The Authors, 838(February), p. 155828. doi: 10.1016/j.scitotenv.2022.155828.

Robins, P. E. *et al.* (2022) 'Predicting the dispersal of SARS-CoV-2 RNA from the wastewater treatment plant to the coast', *Heliyon*. The Authors, 8(9), p. e10547. doi: 10.1016/j.heliyon.2022.e10547.

La Rosa, G. *et al.* (2020) 'Coronavirus in water environments: Occurrence, persistence and concentration methods - A scoping review', *Water Research*. Elsevier Ltd, 179, p. 115899. doi: 10.1016/j.watres.2020.115899.

Rzezutka, A. and Cook, N. (2004) 'Survival of human enteric viruses in the environment and food', *FEMS Microbiology Reviews*, 28(4), pp. 441–453. doi: 10.1016/j.femsre.2004.02.001.

Sala-Comorera, L. *et al.* (2021) 'Decay of infectious SARS-CoV-2 and surrogates in aquatic environments', *Water Research*. Elsevier Ltd, 201, p. 117090. doi: 10.1016/j.watres.2021.117090.

Santiana, M. *et al.* (2018) 'Vesicle-Cloaked Virus Clusters Are Optimal Units for Inter-organismal Viral Transmission', *Cell Host and Microbe*, 24(2), pp. 208-220.e8. doi: 10.1016/j.chom.2018.07.006.

Scherer, K. M. *et al.* (2021) 'Fluorescent reporter system enables spatiotemporal analysis of host cell modi fi cation during herpes simplex virus-1 replication', *Journal of Biological Chemistry*. Elsevier B.V, 296, pp. 1–16. doi: 10.1074/jbc.RA120.016571.

Shang, J. *et al.* (2020) 'Structure of mouse coronavirus spike protein complexed with

572 receptor reveals mechanism for viral entry', *PLoS Pathogens*, 16(3), pp. 1–20. doi:
573 10.1371/journal.ppat.1008392.

574 Sherchan, S. *et al.* (2023) 'Survival of SARS-CoV-2 in wastewater', *Science of the Total*
575 *Environment*. Elsevier B.V., 882(February), p. 163049. doi: 10.1016/j.scitotenv.2023.163049.

576 Skraber, S. *et al.* (2007) 'Occurrence and persistence of bacterial and viral faecal indicators
577 in wastewater biofilms', *Water Science and Technology*, 55(8–9), pp. 377–385. doi:
578 10.2166/wst.2007.280.

579 Smit, J. *et al.* (2023) *Social and Economic Consequences of COVID-19*.

580 Uisce Water (2021) *Annual Environmental Report (Ringsend)*.

581 V'kovski, P. *et al.* (2021) 'Coronavirus biology and replication: implications for SARS-CoV-2',
582 *Nature Reviews Microbiology*. Springer US, 19(3), pp. 155–170. doi: 10.1038/s41579-020-
583 00468-6.

584 Weidhaas, J. *et al.* (2021) 'Correlation of SARS-CoV-2 RNA in wastewater with COVID-19
585 disease burden in sewersheds', *Science of The Total Environment*, 775(June). doi:
586 10.1016/j.scitotenv.2021.145790.

587 Wurtzer, S. *et al.* (2021) 'Several forms of SARS-CoV-2 RNA can be detected in wastewaters:
588 Implication for wastewater-based epidemiology and risk assessment', *Water Research*.
589 Elsevier Ltd, 198, p. 117183. doi: 10.1016/j.watres.2021.117183.

590 Xia, B. *et al.* (2023) 'Extracellular vesicles mediate antibody-resistant transmission of SARS-
591 CoV-2', *Cell Discovery*. Springer US, 9(1). doi: 10.1038/s41421-022-00510-2.

592 Ye, Y. *et al.* (2016) 'Survivability, Partitioning, and Recovery of Enveloped Viruses in

593 Untreated Municipal Wastewater', *Environmental Science and Technology*, 50(10), pp.

594 5077–5085. doi: 10.1021/acs.est.6b00876.

595

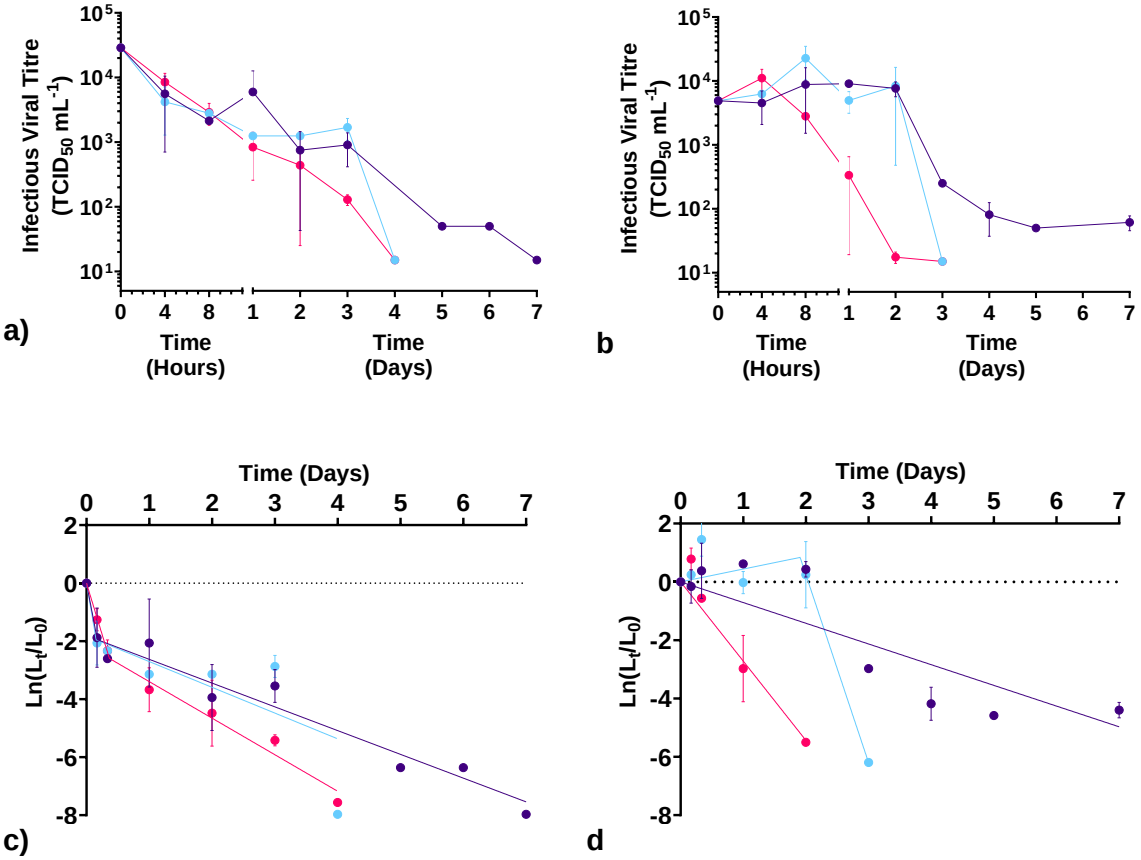

Figure 1. Decay over time of infectious a) SARS-CoV-2 and b) MHV in wastewater as determined by $TCID_{50}$ = median tissue culture infectivity dose. The mean decay curves of infectious c) SARS-CoV-2 and d) MHV in wastewater, where the natural log (Ln)-transformed infectious titre at each time point (L_t) was divided by the initial concentration (L_0). Line colours are indicative of microcosm incubations at 4 °C (●), 10 °C (●) and room temperature (●). Data points indicate mean values obtained from duplicate experiments, with error bars representing standard deviation (n = 8).

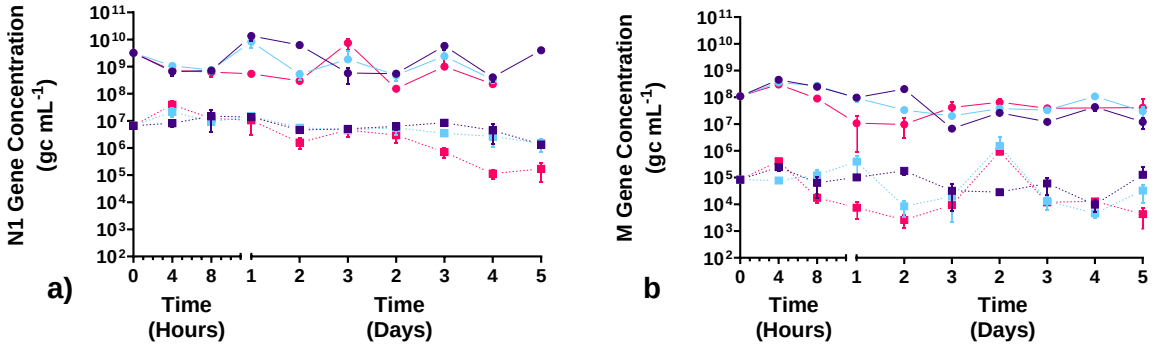

Figure 2. Total (circles on solid lines) and PMA-treated (squares on dashed lines) RNA of a) SARS-CoV-2 N1 gene and b) MHV M gene in wastewater at 4 °C (●) , 10 °C (●) and room temperature (●). Data points indicate mean values obtained from duplicate experiments, with error bars representing standard deviation (n = 6).

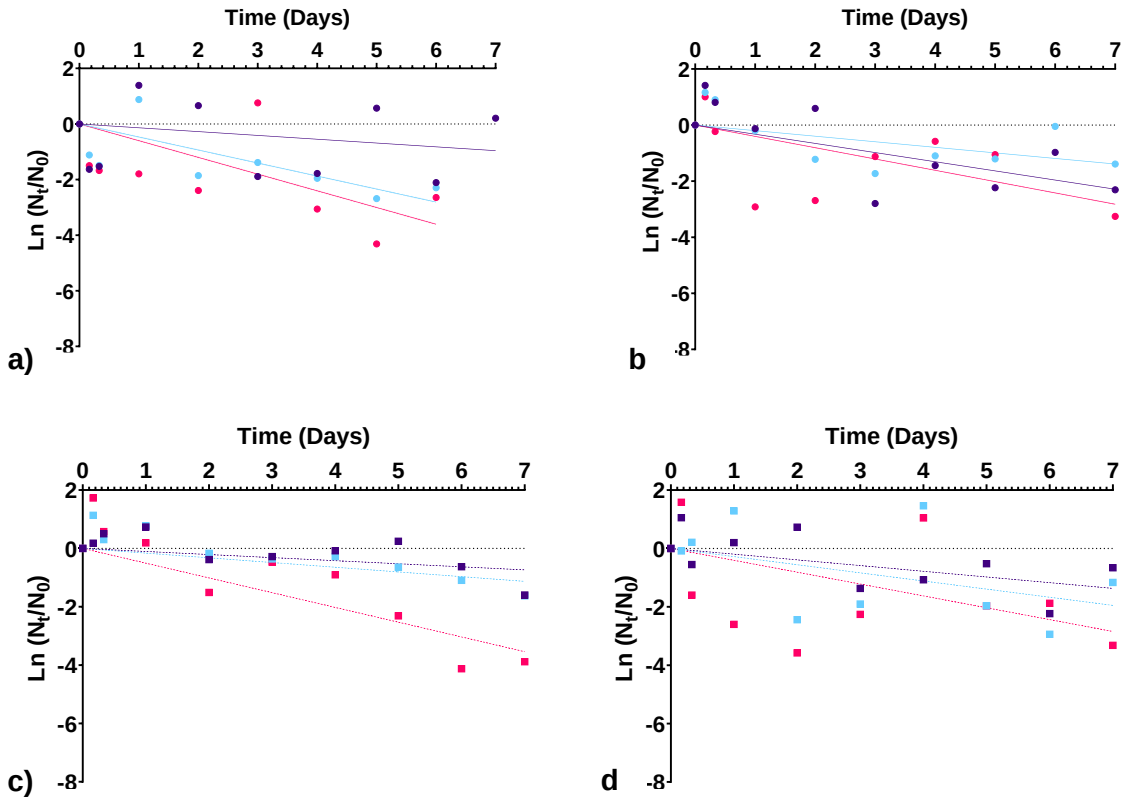

Figure 3. Decay curves of total RNA (circles on solid lines) of a) SARS-CoV-2 and b) MHV in wastewater, and decay curves of PMA-treated RNA (squares on dashed lines) of c) SARS-CoV-2 and d) MHV in wastewater. Line colours are indicative of microcosm incubations at 4 °C (●) , 10 °C (●) and room temperature (●). Data points indicate mean values obtained from duplicate experiments, with error bars representing standard deviation (n = 6).

Table 1. Decay model results of infectious SARS-CoV-2 and MHV decay ($TCID_{50}$) by virus and condition. s: stable for duration (7 days) of experiment.

Virus	Conditions	No. of phases	Phase 1				Phase 2				r^2	RMSE	AICc
			Slope 1 (95% CI)	T_{90} (Hours; 95% CI)	T_{90} (Days; 95% CI)	Decay Rate (day^{-1}; 95% CI)	Slope 2 (95% CI)	T_{90} (Hours; 95% CI)	T_{90} (Days; 95% CI)	Decay Rate (day^{-1}; 95% CI)			
SARS-CoV-2	4 °C	2	-0.47 (s to -0.20)	4.9 (s to 11.3)	0.20 (s to 0.47)	9.55 ± 3.97 (5.58 to 13.5)	-0.03 (-0.04 to -0.02)	67.5 (51.8 to 96.8)	2.81 (2.16 to 4.03)	1.54 ± 0.477 (1.06 to 2.02)	0.9	0.8	2.9
	10 °C	2	-0.53 (s to -0.25)	4.4 (s to 9.1)	0.18 (s to 0.38)	9.7 ± 3.99 (5.71 to 13.7)	-0.04 (-0.06 to -0.01)	62.3 (36.2 to 222.3)	2.59 (1.51 to 9.26)	1.89 ± 0.578 (1.31 to 2.47)	0.7	1.1	13.6
	Room Temperature	2	-0.30 (-0.48 to -0.21)	7.8 (4.8 to 11.1)	0.32 (0.19 to 0.46)	6.08 ± 1.79 (4.29 to 7.87)	-0.05 (-0.07 to -0.04)	43.9 (33.8 to 62.6)	1.83 (1.41 to 2.61)	1.98 ± 0.245 (1.73 to 2.23)	1.0	0.5	-8.1
Murine hepatitis virus	4 °C	1	-0.03 (-0.05 to -0.02)	77.8 (49.0 to 101.4)	3.24 (2.04 to 4.22)	0.236 ± 0.78 (s to 1.02)	--	--	--	--	0.8	1.1	7.5
	10 °C	2	0.02 (-0.02 to 0.07)	s	s	s	-0.27 (-0.37 to -0.17)	8.6 (6.3 to 13.6)	0.36 (0.26 to 0.57)	1.9 ± 0 (1.9 to 1.9)	0.9	0.8	7.3
	Room Temperature	1	-0.11 (-0.14 to -0.08)	20.3 (16.1 to 27.6)	0.85 (0.67 to 1.15)	0.844 ± 2.16 (s to 3)	--	--	--	--	0.9	0.8	0.4

Table 2. Decay model results of RT-qPCR data by virus, condition and PMA-treatment.

Virus	Conditions	No. of phases	Phase 1			Phase 2			r^2	RMSE	AICc
			Slope 1 (95% CI)	T_{90} (Days; 95% CI)	Decay Rate (day^{-1}; 95% CI)	Slope 2 (95% CI)	T_{90} (Days; 95% CI)	Decay Rate (day^{-1}; 95% CI)			
SARS-CoV-2	4 °C	2	-0.47 (s to -0.20)	0.20 (s to 0.47)	9.55 ± 3.97 (5.58 to 13.5)	-0.03 (-0.04 to -0.02)	2.81 (2.16 to 4.03)	1.54 ± 0.477 (1.06 to 2.02)	0.9	0.8	2.9
	10 °C	2	-0.53 (s to -0.25)	0.18 (s to 0.38)	9.7 ± 3.99 (5.71 to 13.7)	-0.04 (-0.06 to -0.01)	2.59 (1.51 to 9.26)	1.89 ± 0.578 (1.31 to 2.47)	0.7	1.1	13.6
	Room Temperature	2	-0.30 (-0.48 to -0.21)	0.32 (0.19 to 0.46)	6.08 ± 1.79 (4.29 to 7.87)	-0.05 (-0.07 to -0.04)	1.83 (1.41 to 2.61)	1.98 ± 0.245 (1.73 to 2.23)	1.0	0.5	-8.1
Murine hepatitis virus	4 °C	1	-0.03 (-0.05 to -0.02)	3.24 (2.04 to 4.22)	0.236 ± 0.78 (s to 1.02)	--	--	--	0.8	1.1	7.5
	10 °C	2	0.02 (-0.02 to 0.07)	s	s	-0.27 (-0.37 to -0.17)	0.36 (0.26 to 0.57)	1.9 ± 0 (1.9 to 1.9)	0.9	0.8	7.3
	Room Temperature	1	-0.11 (-0.14 to -0.08)	0.85 (0.67 to 1.15)	0.844 ± 2.16 (s to 3)	--	--	--	0.9	0.8	0.4

Table 3. Summary of comparison analysis of concentration decay kinetics and T_{90} values for both viruses (PMA-treated and untreated). ns = non-significant.

Data	Temperature	Kruskal-Wallis test (*p value)*
RT-qPCR (RNA)	4	ns
	10	< 0.1
	Room Temperature	< 0.01
RT-qPCR (PMA-treated RNA)	4	ns
	10	ns
	Room Temperature	< 0.01

Supplementary Table 1. PCR primer and probe sequences

Target Gene	Primer/Probe Sequence (5' – 3')	Primer/Probe Concentration	Cycling Conditions	Reference
SARS-CoV-2 Nucleocapsid 1	**Forward (F)**: GACCCCAAAATCAGCGAAAT **Reverse (R):** TCTGGTTACTGCCAGTTGAATCTG **Probe (P):** ACCCCGCATTACGTTTGGTGGACC	500 nM (F) 500 nM (R) 125 nM (P)	RT (50 °C – 600 s), 95 °C – 30 s, 45 cycles (95 °C – 5s, 60 °C – 30 s)	(Lu *et al.*, 2020)
MHV Membrane	**Forward (F):** GGAACTTCTCGTTGGGCATTATACT **Reverse (R):** ACCACAAGATTATCATTTTCACAACATA **Probe (P):** ACATGCTACGGCTCGTGTAACCGAACTGT	300 nM (F) 300 nM (R) 125 nM (P)	RT (50 °C – 600 s), 95 °C – 30 s, 45 cycles (95 °C – 15s, 60 °C – 60 s)	(Besselsen, Wagner and Loganbill, 2002)

Declaration of Interest Statement

The authors declare that they have no known competing financial interests or personal relationships that could have appeared to influence the work reported in this paper.

Author Contributions Statement

KP, LJR, LSC, WM and NF designed the experiments. KP and LJR carried out initial experimentation. KP and NF set up the microcosm. KP carried out RNA extractions, performed RT-PCRs and TCID50 assays. All authors contributed to data analysis. All authors contributed to the article and approved the submitted version.